

# Lawrence Berkeley National Laboratory

## LBL Publications

### Title

Seeded stimulated X-ray emission at 5.9 keV.

### Permalink

<https://escholarship.org/uc/item/3vt0g6n0>

### Journal

Optica, 10(4)

### ISSN

2334-2536

### Authors

Doyle, Margaret D  
Halavanau, Aliaksei  
Zhang, Yu  
et al.

### Publication Date

2023-04-20

### DOI

10.1364/optica.485989


### Copyright Information

This work is made available under the terms of a Creative Commons Attribution License, available at <https://creativecommons.org/licenses/by/4.0/>

Peer reviewed



# Seeded stimulated X-ray emission at 5.9 keV

MARGARET D. DOYLE,<sup>1,†</sup> ALIAKSEI HALAVANAU,<sup>2,†</sup> YU ZHANG,<sup>3</sup> YURINA MICHINE,<sup>4</sup> JOSHUA EVERTS,<sup>5,6</sup> FRANKLIN FULLER,<sup>7</sup> ROBERTO ALONSO-MORI,<sup>7</sup> MAKINA YABASHI,<sup>8,9</sup> ICHIRO INOUE,<sup>8</sup> TAITO OSAKA,<sup>8</sup> JUMPEI YAMADA,<sup>8</sup> YUICHI INUBUSHI,<sup>8,9</sup> TORU HARA,<sup>8</sup> JAN KERN,<sup>1</sup> JUNKO YANO,<sup>1</sup> VITTAL K. YACHANDRA,<sup>1</sup> NINA ROHRINGER,<sup>10,11</sup> HITOKI YONEDA,<sup>4</sup> THOMAS KROLL,<sup>5</sup> CLAUDIO PELLEGRINI,<sup>2</sup> AND UWE BERGMANN<sup>3,12,\*</sup> 

<sup>1</sup>Molecular Biophysics and Integrated Bioimaging Division, Lawrence Berkeley National Laboratory, Berkeley, California 94720, USA

<sup>2</sup>Accelerator Research Division, SLAC National Accelerator Laboratory, Menlo Park, California 94025, USA

<sup>3</sup>Stanford PULSE Institute, SLAC National Accelerator Laboratory, Menlo Park, California 94025, USA

<sup>4</sup>Institute for Laser Science, The University of Electro-Communications, Chofu, Tokyo 182-8585, Japan

<sup>5</sup>Stanford Synchrotron Radiation Lightsource, SLAC National Accelerator Laboratory, Menlo Park, California 9402, USA

<sup>6</sup>Department of Physics, University of Chicago, Chicago, Illinois 60637, USA

<sup>7</sup>Linac Coherent Light Source, SLAC National Accelerator Laboratory, Menlo Park, California 94025, USA

<sup>8</sup>RIKEN SPring-8 Center, Sayo-cho, Sayo-gun, Hyogo 679-5148, Japan

<sup>9</sup>Japan Synchrotron Radiation Research Institute, Sayo-cho, Sayo-gun, Hyogo 679-5198, Japan

<sup>10</sup>Center for Free-Electron Laser Science CFEL, Deutsches Elektronen-Synchrotron DESY, Hamburg 22607, Germany

<sup>11</sup>Department of Physics, Universität Hamburg, Hamburg 20355, Germany

<sup>12</sup>Department of Physics, University of Wisconsin-Madison, Madison, Wisconsin 53706, USA

<sup>†</sup>These authors contributed equally to this paper.

\*ubergmann@wisc.edu

Received 18 January 2023; revised 11 March 2023; accepted 27 March 2023; published 17 April 2023

X-ray free-electron lasers (XFELs) provide intense pulses that can generate stimulated X-ray emission, a phenomenon that has been observed and studied in materials ranging from neon to copper. Two schemes have been employed: amplified spontaneous emission (ASE) and seeded stimulated emission (SSE), where a second color XFEL pulse provides the seed. Both phenomena are currently explored for coherent X-ray laser sources and spectroscopy. Here, we report measurements of ASE and SSE of the 5.9 keV Mn  $K\alpha_1$  fluorescence line from a 3.9 molar  $\text{NaMnO}_4$  solution, pumped with 7 femtosecond FWHM XFEL pulses at 6.6 keV. We observed ASE at a pump pulse intensity of  $1.7 \times 10^{19} \text{ W/cm}^2$ , consistent with earlier findings. We observed SSE at dramatically reduced pump pulse intensities down to  $1.1 \times 10^{17} \text{ W/cm}^2$ . These intensities are well within the range of many existing XFEL instruments, which supports the experimental feasibility of SSE as a tool to generate coherent X-ray pulses, spectroscopic studies of transition metal complexes, and other applications. © 2023 Optica Publishing Group under the terms of the [Optica Open Access Publishing Agreement](#)

<https://doi.org/10.1364/OPTICA.485989>

## 1. INTRODUCTION

The advent of the X-ray free-electron laser (XFEL) [1] has made possible the exploration of many femtosecond-angstrom scale physics phenomena that were previously unobservable [2,3]. One such phenomenon is stimulated X-ray emission, first observed in the form of inner-shell lasing for the neon  $K\alpha$  line at 850 eV [4] and then for the copper  $K\alpha$  line at 8 keV [5]. Stimulated emission can occur by amplified spontaneous emission (ASE) using an XFEL pump pulse [4,6,7] and seeded stimulated emission (SSE) using a two-color XFEL pump and seed pulse [5,8]. The collectively emitted photons (e.g., at the Ne, Mn, and Cu  $K\alpha_1$  lines), can exhibit high levels of coherence and spectral resolution [6,8,9]. Several applications of ASE and SSE are currently under investigation, including novel X-ray spectroscopy probes with potentially enhanced chemical sensitivity [6,8] and the generation of new

coherent X-ray sources with properties beyond those provided by XFEL pulses [4,5,9–11].

XFEL pulses are based on self-amplified spontaneous emission (SASE) [12], which results in limited coherence, temporal and spectral spikes [13], and large intensity fluctuations. Techniques to improve the pulse properties include self-seeding [14–18], fresh slice/bunch seeding [19,20], and the conventional approach of frequency filtering the pulses with a monochromator.

While externally seeded FELs can produce nearly fully coherent [21] and stable pulses, and there are proposed schemes to increase the stability of FELs [22], high-gain, single-pass sources like XFELs have inherent stochastic fluctuations that limit the generation of stable, fully coherent, transform-limited pulses in the hard X-ray regime. This requires a multipass cavity-based system such as, for example, an XFEL oscillator [23,24]. Stimulated X-ray emission is at the heart of a different multipass cavity-based approach to

generate intense, stable, transform-limited, femtosecond X-ray pulses. The proposed population inversion X-ray laser oscillator (XLO) [11] uses a two-stage process where the XFEL pulse generates stimulated  $K\alpha$  X-ray emission in a gain medium. The XLO operates with a train of intense XFEL pulses and uses an X-ray optical Bragg cavity to recirculate the stimulated X-ray emission pulses. Critical parameters of the XLO are the pump and seed pulse intensities and the amplification factor (gain) obtained at each cavity passage. Provided that one can achieve an adequate temporal and spatial overlap of pump and seed pulses, the gain is primarily dependent on the pump and seed pulse intensity, the gain medium concentration and thickness, and the number of excited atoms. These parameters are also critical when considering stimulated X-ray emission for spectroscopy applications on transition metal complexes [6,8] or for the generation of phase-stable femtosecond X-ray pulse pairs [9]. The general aim is to obtain stimulated X-ray emission at the lowest possible pump pulse intensity because this facilitates the rapid gain medium replacement required for an XLO (a cavity length of  $\sim 10$  m corresponds to a pulse spacing of  $\sim 33$  ns). A lower pump pulse intensity also reduces X-ray-induced electronic structure changes for spectroscopy applications [25,26].

In this paper we report a systematic study that establishes the parameters to minimize the pump pulse intensity for stimulated X-ray emission. It was accomplished by splitting the XFEL undulator in two parts: one tuned to the pump pulse photon energy and the other to the seed pulse photon energy. We measured stimulated X-ray emission at the Mn  $K\alpha$  line in a 3.9 molar  $\text{NaMnO}_4$  solution, where we varied the pulse parameters over more than two orders of magnitude. We have provided the calculations of pump and seed pulse intensities based on the measured signals and our results can be straightforwardly extrapolated to other emission lines, various gain medium and sample concentrations and thicknesses, as well as XFEL parameters. They provide a benchmark for various applications of the exciting phenomenon of stimulated X-ray emission.

## 2. EXPERIMENTAL SETUP

The experiments were performed at the SACLA XFEL facility at Experimental Hutch 5 (EH5), as shown in Fig. 1(a). The SACLA XFEL was configured in two-color mode [27,28]. The first seven undulators were used to generate the seed pulses at the 5.9 keV Mn  $K\alpha_1$  photon energy. These SASE pulses were filtered through a Si (111) channel-cut Bragg crystal, to provide monochromatic seed pulses with  $<1$  eV FWHM. The exact number changes slightly on a shot-by-shot basis depending on the beam condition upstream of the monochromator. The 14 downstream undulators produced the 7 fs FWHM SASE pump pulses at 6.6 keV, above the Mn K edge [29–31]. The two-color pulses were focused with Kirkpatrick–Baez (KB) mirrors [31–33] to a 120 nm (horizontal) by 180 nm (vertical) FWHM spot size, as determined by knife-edge scans. The beam divergence downstream of the focus was 3.8 mrad (horizontal) and 1.9 mrad (vertical).

The gain medium was a concentrated sodium permanganate ( $\text{NaMnO}_4$ ) solution (3.9 molar Mn) delivered in a liquid jet, with a 100  $\mu\text{m}$  diameter, located inside a helium-filled vacuum chamber. The nozzle and the recirculating pump system for the jet was designed at SACLA [34]. The estimated pump pulse energy at the gain medium was 40  $\mu\text{J}$ , corresponding to an intensity of  $1.7 \times 10^{19}$  W/cm<sup>2</sup>, when the gain medium was fully in focus. For a conceptual figure behind how both pump and seed pulses

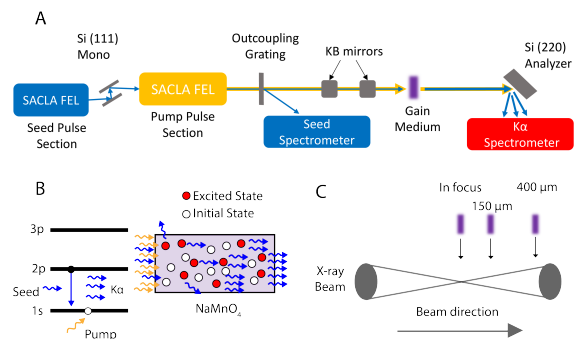


**Fig. 1.** (a) Experimental layout (not to scale): SACLA XFEL radiation containing the seed and pump pulses is focused with a KB mirror system onto a liquid jet of  $\text{NaMnO}_4$ . 2% of the seed pulse is outcoupled and registered in the seed spectrometer. The resulting stimulated emission is dispersed onto the  $K\alpha$  spectrometer with a Si (220) crystal analyzer. (b) The level diagram and concept behind SSE. The pump pulse (yellow), which is tuned above the Mn K edge, creates a population inverted 1s core hole excited state. The seed pulse (blue) is tuned to the  $K\alpha$  emission line to seed the SSE signal (red). (c) Schematic showing how the pump and seed pulse intensity is varied by moving the gain medium to various distances out of focus along the beam direction.

participated in the SSE process in the  $\text{NaMnO}_4$  solution, see Fig. 1(b).

The seed pulse spectra were analyzed with a 2% sampling grating followed by a dispersive spectrometer consisting of an elliptical mirror, Si (111) analyzer crystal, and a 2D multiport CCD (MPCCD) detector located in the experimental hutch 1 (EH1) [35], referred to as the seed spectrometer, as shown in Fig. 1(a). The ASE and SSE spectra were analyzed with a flat Si (220) analyzer crystal reflecting the beam in the horizontal plane onto a second 2D MPCCD detector [9], the  $K\alpha$  spectrometer, as shown in Fig. 1(a). For measurements where the jet was moved 150, 500, and 600  $\mu\text{m}$  out of focus along the beam direction, a 25  $\mu\text{m}$  thick aluminum foil was placed in front of the  $K\alpha$  spectrometer. With this configuration, we recorded the seed pulse and the SSE spectra simultaneously, shot-by-shot. All relevant transmission factors from the experimental setup are listed in Table 1.

**Table 1. Relevant Experimental Components and Their Corresponding Transmission Factors at 5.9 keV (Used to Correct for the Number of Photons at the Gain Medium)**

Component	Thickness	Transmission (%)
KB Be windows	200 $\mu\text{m}$	91
KB reflectivity	N/A	80
Kapton windows	150 $\mu\text{m}$	56
Aluminum foil	25 $\mu\text{m}$	46
X-ray transport losses	N/A	45
Air path after gain medium	35 cm	36
Si (220) analyzer	N/A	1 <sup>a</sup>

<sup>a</sup>Resulting from the ratio of horizontal beam divergence (3.8 mrad) and Si (220) Darwin width (27  $\mu\text{rad}$ ).

NOTE: The only losses relevant to the seed spectrometer come from the X-ray transport losses and KB reflectivity. The remaining elements in the table are used to correct the  $K\alpha$  spectrometer.

**Table 2. Distance from Nanofocus, Horizontal ( $x$ ), and Vertical ( $y$ ) Beam Size at the Gain Medium<sup>a</sup>**

Distance Out of Focus ( $\mu\text{m}$ )	$x$ (nm) FWHM	$y$ (nm) FWHM	$I_{\text{pump}}$ ( $\text{W}/\text{cm}^2$ )	$I_{\text{seed}}$ ( $\text{W}/\text{cm}^2$ ) ( $\delta E = 0$ eV)	$I_{\text{seed}}$ ( $\text{W}/\text{cm}^2$ ) ( $\delta E = 7$ eV)
0	120	180	$1.7 \times 10^{19}$	$3.2 \times 10^{15}$	$7.9 \times 10^{12}$
150	690	465	$1.1 \times 10^{18}$	$2.2 \times 10^{14}$	$5.3 \times 10^{11}$
300	1260	750	$3.8 \times 10^{17}$	$7.4 \times 10^{13}$	$1.8 \times 10^{11}$
400	1640	940	$2.4 \times 10^{17}$	$4.5 \times 10^{13}$	$1.1 \times 10^{11}$
500	2020	1130	$1.6 \times 10^{17}$	$3.1 \times 10^{13}$	$7.4 \times 10^{10}$
600	2400	1320	$1.1 \times 10^{17}$	$2.2 \times 10^{13}$	$5.4 \times 10^{10}$

<sup>a</sup>Calculated by assuming the 3.8 mrad (horizontal) and 1.9 mrad (vertical) beam divergence downstream of the focus, and the corresponding pump ( $I_{\text{pump}}$ ) and seed ( $I_{\text{seed}}$ ) pulses intensities at the gain medium.

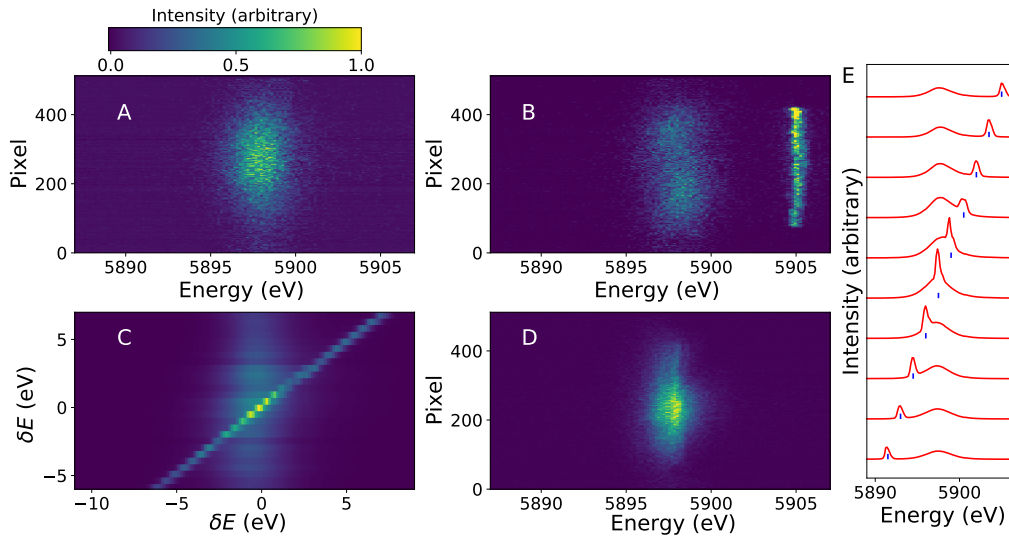


**Fig. 2.** (a) Selected single-shot ASE spectrum collected at a pump intensity of  $1.7 \times 10^{19}$   $\text{W}/\text{cm}^2$ ; single-shot SSE spectrum (center) and seed pulse (right vertical line) at (b)  $\delta E = 7$  eV above  $K\alpha_1$  and (d)  $\delta E = 0$  eV at a pump intensity of  $1.1 \times 10^{18}$   $\text{W}/\text{cm}^2$ ; (c) detuning scan of  $K\alpha_1$  SSE at a pump intensity of  $1.1 \times 10^{18}$   $\text{W}/\text{cm}^2$ , in which each horizontal row corresponds to the average spectrum for a given seed pulse energy collected across 1924 shots and each seed is indicated by a square box on the diagonal; (e) 1D version of (c), showing  $K\alpha_1$  SSE spectra (solid red lines), in which the center of the seed pulse energy is indicated by a blue vertical line. Each 2D spectrum shown was collected at the  $K\alpha$  spectrometer, and is peak normalized. Each 1D spectrum in (e) is normalized to the peak pixel value from (c).

### 3. ESTABLISHING THE PUMP AND SEED PULSE PARAMETERS FOR SSE

Using the same formula as described by Table 1(e) in Fransson *et al.* [26], we estimated the pump and seed pulse intensities, as shown in Table 2. The pump pulse energy at the gain medium was estimated to be 40  $\mu\text{J}$ , as measured by a calibrated inline intensity monitor [32]. For the seed pulse, we base our estimates on the photon counts in regions (a) and (b) of the average seed pulse spectrum shown in Fig. 3, (the photon count in the latter suggests the estimated seed pulse energy at the gain medium to be  $\sim 0.01$   $\mu\text{J}$ ) and the assumption that the beam size of the seed pulse is the same for the cases of a tuned and detuned monochromator. To obtain the intensity, we only considered the photons that fall within the FWHM of the elliptical Gaussian focus, which is 50% of the total [26]. We then divided this by the pulse duration (7 fs) [36] and area (A) under this focus (FWHM)  $A = xy \times \pi/4$ , where  $x$  and  $y$  are the horizontal and vertical beam sizes at the gain medium.

We first placed the jet in focus at the maximum pump pulse intensity  $I_{\text{pump}} = 1.7 \times 10^{19}$   $\text{W}/\text{cm}^2$  to generate Mn  $K\alpha_1$  ASE (without a seed pulse). The corresponding 2D spectrum is shown in Fig. 2(a), in which the spectral direction is shown along the horizontal axis and the spatial direction is shown along the vertical axis. Moving the gain medium 150  $\mu\text{m}$  out of focus reduced the

pump to  $I_{\text{pump}} = 1.1 \times 10^{18}$   $\text{W}/\text{cm}^2$  and resulted in the loss of the ASE signal. This established that the lowest pump pulse intensity to observe ASE from a 3.9 molar  $\text{NaMnO}_4$  solution was between these two values, at some factor times  $10^{18}$   $\text{W}/\text{cm}^2$ . We estimated that the minimum pump pulse intensity to observe ASE from the most concentrated Mn gain medium, such as a 25  $\mu\text{m}$  Mn foil, was a factor of 8 lower, corresponding to four times smaller thickness and 33 times larger concentration (78.9 Mn atoms/ $\text{nm}^3$  for the foil, 2.4 Mn atoms/ $\text{nm}^3$  in solution). This estimate assumes: (i) that the Rayleigh length of the KB mirrors was the same or more than the size of our jet diameter (100  $\mu\text{m}$ ), and (ii) that the onset of stimulated emission occurred when the concentration times pump pulse intensity reached a certain value (e.g., twice the concentration requires half the pump pulse intensity), which is an approximation.

After establishing the pump pulse intensity limit of  $1.1 \times 10^{18}$   $\text{W}/\text{cm}^2$  where no ASE was observed, we added the monochromatic seed pulse and scanned its photon energy through the Mn  $K\alpha_1$  line. We started at  $\delta E = 7$  eV above the Mn  $K\alpha_1$  line, where we already observed SSE, as shown in Fig. 2(b). At this detuning value, only a small fraction of the seed pulse intensity spectrally overlapped with the peak of the Mn  $K\alpha_1$  line (see next section for a detailed discussion). Figure 2(c) shows the heat map

of the complete seed pulse scan, where each horizontal line corresponds to the seed pulse photon energy as it is swept through the Mn  $K\alpha_1$  spectrum. As the seed moved closer to the center of the Mn  $K\alpha_1$  line, there was no strong change in the spectral shape and intensity of the SSE signal. See Fig. 2(e) for the corresponding series of SSE spectra. This indicated that this series of SSE was close to the limit of the gain curve, where a stronger seed pulse does not result in a stronger SSE signal.

Our next step was to align the seed pulse photon energy with the center of the Mn  $K\alpha_1$  line, as shown in Fig. 2(d), and reduce the pump pulse intensity by moving the jet progressively out of focus (downstream) along the beam direction, as shown in Fig. 1(c). Because the pump and seed pulses share the same beam line optics and focus, doing so also simultaneously changed the seed pulse intensity. The highest number of  $K\alpha_1$  photons observed from a single shot of SSE, using the correction coefficients given in Table 1, was  $2.9 \times 10^8$ , using a pump pulse intensity of  $1.1 \times 10^{18}$  W/cm<sup>2</sup> (corresponding to 150  $\mu$ m out of focus, as listed in Table 2) and a seed pulse intensity of  $9.3 \times 10^{14}$  W/cm<sup>2</sup>. For this shot, the seed pulse was detuned by  $\delta E = -0.5$  eV below  $K\alpha_1$ .

An important quantity is the seeding efficiency defined as the photon ratio  $\rho = N_{K\alpha_1} / N_{\text{seed}}$ , where each  $N$  corresponds to the number of photons that fall within the measured  $K\alpha_1$  FWHM of that shot. The experimentally obtainable value of  $\rho$  depends on the exact spatio-temporal overlap of pump and seed and was difficult to estimate for this experiment without more advanced shot-by-shot diagnostics.  $N_{K\alpha_1}$  was determined by subtracting  $N_{\text{seed}}$  [from the first detector, as shown in Fig. 1(a)] from the total photon count registered by the  $K\alpha$  spectrometer in the same bandwidth. The strongest single shot enhancement of  $K\alpha_1$  photons with respect to seed photons within the  $K\alpha_1$  FWHM was  $\rho = 8.4 \times 10^3$ . For this single shot of SSE, the pump and seed pulse intensities were  $1.1 \times 10^{18}$  W/cm<sup>2</sup> and  $2.0 \times 10^{11}$  W/cm<sup>2</sup>, respectively. The low  $I_{\text{seed}}$  comes from the fact that, for this shot, the seed was detuned by  $\delta E = 7$  eV above the  $K\alpha_1$  so that only  $7.6 \times 10^3$  seed photons

were estimated to be found within the  $K\alpha_1$  FWHM. Nevertheless,  $6.4 \times 10^7$   $K\alpha_1$  photons were observed.

After moving to a pump pulse as low as  $I_{\text{pump}} = 1.1 \times 10^{17}$  W/cm<sup>2</sup>, a seed pulse intensity of  $I_{\text{seed}} = 7.8 \times 10^{12}$  W/cm<sup>2</sup> was required to observe a single shot of SSE with  $\rho = 9.8$ , resulting in an estimated  $2.8 \times 10^7$  photons in the  $K\alpha_1$  FWHM. This pump pulse intensity is comparable to or even an order of magnitude lower than typical values used in experiments at XFELs using standard  $\mu$ m focusing optics [26].

We now discuss varying the seed pulse intensity at a constant pump pulse intensity. This can be accomplished by detuning the seed pulse photon energy from the  $K\alpha_1$  peak. Figure 3 shows an average seed pulse spectrum collected across 1924 single shots, placed on a log plot and corrected for the number of photons at the gain medium. For illustrative purposes, two spectral regions with the same bandwidth as the spontaneous NaMnO<sub>4</sub>  $K\alpha_1$  linewidth,  $\Delta E_{K\alpha_1} = 2.1$  eV FWHM [6], were selected to compare photon counts when the seed was tuned directly on top of  $K\alpha_1$ , as shown in Fig. 2(d) and detuned by  $\delta E = 7$  eV from  $K\alpha_1$ ; see Fig. 2(b) for a sample spectrum. Due to the seed's spectral shape, which contains some Lorentzian character, the total photon count in  $\Delta E_{K\alpha_1}$  remained above  $10^4$  photons. It is even true that in cases where the seed was detuned by  $\delta E = 7$  eV, the reduced number of photons (by more than a factor of 400) were still sufficient to stimulate emission.

#### 4. SPECTRAL ANALYSIS AND SEEDING EFFICIENCY

To analyze the spectral characteristics of both the seed pulse and SSE, we projected each detector image onto the energy axis and fit it with a pseudo-Voigt function

$$I(E, f) = I_0 [(1 - \eta)G(E, f) + \eta L(E, f)], \quad (1)$$

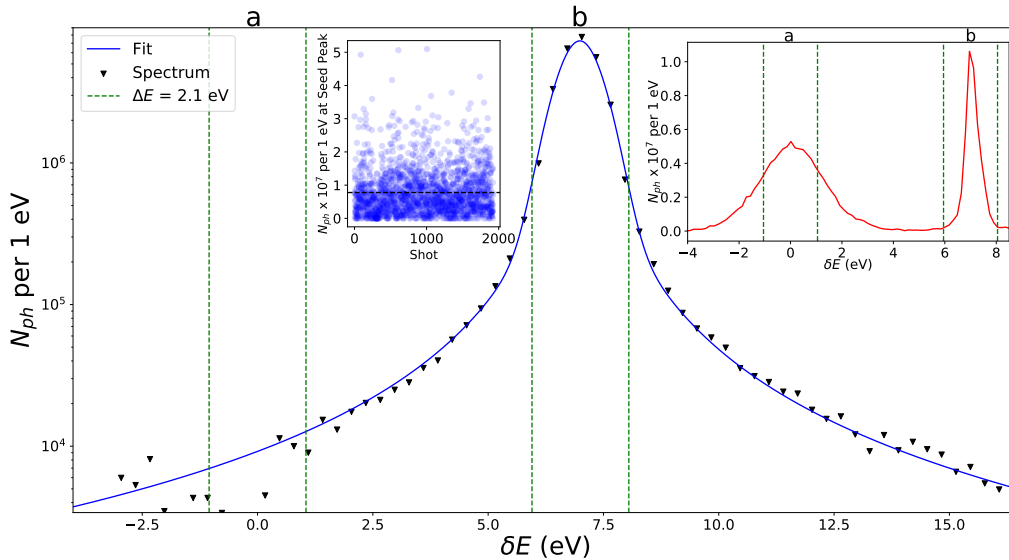


**Fig. 3.** Seed pulse spectrum obtained from averaging 1924 single shots, and the corresponding best fit from Eq. (1). The left inset shows the shot-by-shot seed intensity, which exhibits 100% fluctuation and has an estimated average value of  $7.8 \times 10^6$  (black broken line). The average spectrum and corresponding fit were shifted to  $\delta E = 7$  eV from  $K\alpha_1$  for demonstration purposes. Next, two regions were selected from the shifted fit: (a)  $\delta E = 0$  eV and (b)  $\delta E = 7$  eV. In region (a)  $2.0 \times 10^4$  photons were observed within  $\Delta E_{K\alpha_1} = 2.1$  eV FWHM. In region (b)  $8.2 \times 10^6$  photons were found in a bandwidth of  $\Delta E_{K\alpha_1} = 2.1$  eV FWHM. Integrated photon counts were computed from the fit. The right inset shows the single shot spectrum corresponding to Fig. 2(b) to illustrate how, even in the case of a detuned seed, enough photons from the low-energy tail can stimulate emission.

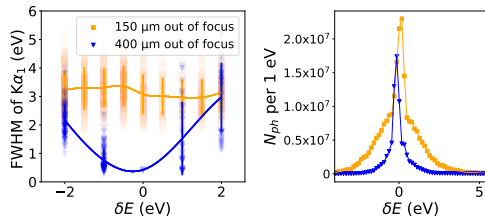


**Fig. 4.** Left: The FWHM,  $f$ , of the Mn  $K\alpha_1$  line as a function of the seed pulse detuning at different pump intensities. Lines are drawn for reference. Right: Example of single-shot spectra, in which the seed is  $\delta E = 0$  eV from the Mn  $K\alpha_1$  line, to further illustrate spectral narrowing.

where  $G(E, f) = \frac{2.355}{f\sqrt{2\pi}} e^{-\frac{1}{2}\left(\frac{2.355 \cdot E}{f}\right)^2}$  is the Gaussian component,  $L(E, f) = \frac{1}{2\pi} \frac{f}{(E^2 + (f/2)^2)}$  is the Lorentzian component,  $E$  is the photon energy,  $f$  is the total FWHM, and  $0 < \eta < 1$  is the Lorentzian parameter [37].

Seed pulse spectra collected at both spectrometers were cross-correlated. Total beamline transmission (from the undulator hall to the target) was found to be 45%. A two-detector setup was necessary to estimate the amount of seed pulse photons in the  $K\alpha_1$  line spectral bandwidth, especially in case of no detuning. When the seed pulse was detuned, one, in principle, can extract the number of seed pulse photons from the spectral fits using only the  $K\alpha$  spectrometer. It has an intrinsic spectral resolution of 0.24 eV FWHM corresponding to the Darwin width of the Si 220 analyzer crystal. Because this is much narrower than most of our spectral features, we did not attempt to deconvolute, and all reported numbers include this broadening. Note that Figs. 4 and 5 show results derived from fitting results with an R-squared value  $> 0.99$ .

At a high pump pulse intensity (150  $\mu\text{m}$  out of focus), we observed a broad spectral width of  $> 3$  eV FWHM with little variation, as shown in Fig. 4. The spectral broadening occurred once SSE reached the saturation regime [6]. In contrast, at a reduced pump pulse intensity (400  $\mu\text{m}$  out of focus) the spectral width of the Mn  $K\alpha_1$  line became narrower when the seed pulse was tuned directly to the resonance, with a minimum width  $< 1$  eV. We assigned the observed narrowing to what in the optical regime is known as gain narrowing [38]. When fitting the signal in the low gain regime with a fixed seed pulse width, the two-component fit overestimated the  $K\alpha_1$  SSE width due to its weak signal. It also overestimated the seed contribution, because in the gain narrowing regime it becomes impossible to differentiate between the spectral contributions from the seed and the  $K\alpha_1$  line. Therefore, the fits represent an upper limit to the  $K\alpha_1$  SSE width.

Figure 5(a) shows the experimentally determined seeding efficiency  $\rho$  as a function of number of seed photons, measured at two different pump intensities (150 and 400  $\mu\text{m}$  out of focus). At high pump pulse intensities, as shown by the yellow squares in Fig. 5(a), the SSE signal was saturated, resulting in a seeding efficiency  $\rho$  that was greatest at low seed pulse intensities. At a lower pump pulse intensity, as shown by the blue triangles in Fig. 5(a), we observed no obvious trend for  $\rho$  as a function of seed photon count.

Because the losses in an XLO cavity are expected to be high [39], the seed pulse intensity will be low; hence, conditions where  $\rho$  is high are required. If an external seed will be used for the initial pass of the XLO, seeding can occur even if the spectral overlap is not yet optimized (i.e., the effective seed pulse intensity is low).

Figure 5(b) indicates that the  $K\alpha_1$  photon number peaks at  $3 \times 10^7$  photons with a lower probability of reaching  $\leq 1 \times 10^7$

photons. The latter fact is likely attributed to the high gain of the atomic medium, when every seed pulse, even with a low photon count, initiated the lasing process. The seed pulse, in turn, exhibited close to negative exponential statistics attributed to the SASE pulse filtered through a monochromator.

## 5. CONCLUSION

To summarize our findings, the lowest pump pulse intensity at which we observed a single shot of SSE at the Mn  $K\alpha_1$  line from a 3.9 molar  $\text{NaMnO}_4$  solution was  $1.1 \times 10^{17}$  W/cm<sup>2</sup>, which was three orders of magnitude lower than previously reported ASE results using the same sample [6]. For this case, a seed pulse with intensity  $7.8 \times 10^{12}$  W/cm<sup>2</sup> was used and the seeding efficiency was  $\rho = 9.8$ . Using our approximation that 50% of the photons fall within the FWHM of a 2D Gaussian focus, a pump pulse intensity of  $10^{17}$  W/cm<sup>2</sup> can be achieved by focusing an XFEL pulse with 1 mJ pulse energy and 7 fs pulse length to a diameter of 9  $\mu\text{m}$  FWHM. This and comparable parameters are routinely achieved at all existing XFELs, and the intensity requirement can be further relaxed when using more concentrated gain media or samples. The highest pump pulse intensities currently available at XFELs are  $> 10^{20}$  W/cm<sup>2</sup>, suggesting that SSE could be applied to transition metal solutions in the several millimolar range.

This shows the feasibility of carrying out seeded stimulated X-ray emission, which is an emerging field with the potential to develop new nonlinear X-ray spectroscopy methods and generate transform-limited femtosecond X-ray pulses.

Our highest single-shot gain resulting in a seeding efficiency of ( $\rho = 8.4 \times 10^3$ ) was achieved using a pump pulse intensity of  $1.1 \times 10^{18}$  W/cm<sup>2</sup> and a seed pulse intensity of  $2.0 \times 10^{11}$  W/cm<sup>2</sup>. This is sufficient to overcome the estimated loss in the first round trip of the proposed XLO [11]. The gain almost disappeared below a pump pulse intensity of  $2.4 \times 10^{17}$  W/cm<sup>2</sup> (400  $\mu\text{m}$  out of focus) corresponding to an estimated pump spot size of 1.2  $\mu\text{m}^2$  FWHM. The largest number of  $K\alpha_1$  photons observed in a single shot was  $2.9 \times 10^8$ , resulting from a pump pulse intensity of  $1.1 \times 10^{18}$  W/cm<sup>2</sup> and a seed pulse intensity of  $9.3 \times 10^{14}$  W/cm<sup>2</sup>. Because this number scales with the total number of population inverted atoms, it can be further increased by increasing the beam diameter of the pump and seed pulses, while providing the same intensity. This requires a larger XFEL pulse energy than we employed at SACLA. Such pulse energies in the mJ range are available, for example, at the LCLS and European XFEL.

When removing the seed pulse, ASE was observed at a pump pulse intensity of  $1.7 \times 10^{19}$  W/cm<sup>2</sup>. We estimate that the maximally concentrated Mn foil, ASE/SSE can be observed from pump and seed pulse intensity reduced by a factor of 8. The average FWHM from the measured SSE spectra collected at a given seed pulse energy range from  $\sim 0.4$  to 3.4 eV, which compares to the spontaneous  $\text{NaMnO}_4$   $K\alpha_1$  linewidth of 2.1 eV FWHM [6].

**Funding.** Japan Society for the Promotion of Science (19K20604, 22H03877); National Institutes of Health (F32GM116423, GM055302, GM110501, GM126289, P41GM103393); U.S. Department of Energy (DE-AC02-05CH11231, DE-AC02-76F00515, DE-AC02-76SF00515).

**Acknowledgment.** A.H., C.P., and U.B. are supported by the U.S. Department of Energy. The experiment at SACLA was performed with the approval of the Japan Synchrotron Radiation Research Institute (proposal no. 2017B8066). Part of this work was supported by the Department of Energy (DOE), Laboratory Directed Research and Development Program at SLAC

National Accelerator Laboratory (to U.B.). Additionally, part of this work was supported by Ruth L. Kirschstein National Research Service Award (to F.D.F.); Director, Office of Science, Office of Basic Energy Sciences, Division of Chemical Sciences, Geosciences, and Biosciences of the DOE Contracts (to C.P., J.Y., V.K.Y., and J.K.); and NIH (to J.K., J.Y., V.K.Y.). This work was supported by JPSJ KAKENHI (to I.I.). The Stanford Synchrotron Radiation Lightsource Structural Molecular Biology Program is supported by the DOE Office of Biological and Environmental Research and NIH National Institute of General Medical Sciences (NIGMS). The contents of this publication are solely the responsibility of the authors and do not necessarily represent the official views of the NIGMS or the NIH.

**Disclosures.** The authors declare no conflicts of interest.

**Data availability.** Data underlying the results presented in this paper are not publicly available at this time but may be obtained from the authors upon reasonable request.

## REFERENCES

- C. Pellegrini, "X-ray free-electron lasers: from dreams to reality," *Phys. Scr.* **2016**, 014004 (2017).
- C. Bostedt, S. Boutet, D. M. Fritz, Z. Huang, H. J. Lee, H. T. Lemke, A. Robert, W. F. Schlotter, J. J. Turner, and G. J. Williams, "Linac coherent light source: The first five years," *Rev. Mod. Phys.* **88**, 015007 (2016).
- U. Bergmann, V. K. Yachandra, and J. Yano, *X-ray Free Electron Lasers: Applications in Materials, Chemistry and Biology* (Royal Society of Chemistry, 2017), Vol. **18**.
- N. Rohringer, D. Ryan, R. A. London, M. Purvis, F. Albert, J. Dunn, J. D. Bozek, C. Bostedt, A. Graf, R. Hill, S. P. Hau-Riege, and J. J. Rocca, "Atomic inner-shell X-ray laser at 1.46 nanometres pumped by an X-ray free-electron laser," *Nature* **481**, 488–491 (2012).
- H. Yoneda, Y. Inubushi, K. Nagamine, Y. Michine, H. Ohashi, H. Yumoto, K. Yamauchi, H. Mimura, H. Kitamura, T. Katayama, T. Ishikawa, and M. Yabashi, "Atomic inner-shell laser at 1.5-ångström wavelength pumped by an X-ray free-electron laser," *Nature* **524**, 446–449 (2015).
- T. Kroll, C. Weninger, R. Alonso-Mori, *et al.*, "Stimulated x-ray emission spectroscopy in transition metal complexes," *Phys. Rev. Lett.* **120**, 133203 (2018).
- M. Beye, S. Schreck, F. Sorgenfrei, C. Trabant, N. Pontius, C. Schüßler-Langeheine, W. Wurth, and A. Föhlisch, "Stimulated X-ray emission for materials science," *Nature* **501**, 191–194 (2013).
- T. Kroll, C. Weninger, F. D. Fuller, *et al.*, "Observation of seeded Mn K $\beta$  stimulated x-ray emission using two-color x-ray free-electron laser pulses," *Phys. Rev. Lett.* **125**, 037404 (2020).
- Y. Zhang, T. Kroll, C. Weninger, *et al.*, "Generation of intense phase-stable femtosecond hard X-ray pulse pairs," *Proc. Natl. Acad. Sci. USA* **119**, e2119616119 (2022).
- C. Weninger and N. Rohringer, "Transient-gain photoionization x-ray laser," *Phys. Rev. A* **90**, 063828 (2014).
- A. Halavanau, A. Benediktovitch, A. Lutman, D. DePonte, D. Cocco, N. Rohringer, U. Bergmann, and C. Pellegrini, "Population inversion X-ray laser oscillator," *Proc. Natl. Acad. Sci. USA* **117**, 15511–15516 (2020).
- R. Bonifacio, C. Pellegrini, and L. Narducci, "Collective instabilities and high gain regime in a free electron laser," *Opt. Commun.* **50**, 373–378 (1984).
- R. Bonifacio, L. De Salvo, P. Pierini, N. Piovella, and C. Pellegrini, "Spectrum, temporal structure, and fluctuations in a high-gain free-electron laser starting from noise," *Phys. Rev. Lett.* **73**, 70 (1994).
- C. Pellegrini, A. Marinelli, and S. Reiche, "The physics of x-ray free-electron lasers," *Rev. Mod. Phys.* **88**, 015006 (2016).
- D. Ratner, R. Abela, J. Amann, *et al.*, "Experimental demonstration of a soft x-ray self-seeded free-electron laser," *Phys. Rev. Lett.* **114**, 054801 (2015).
- L. H. Yu, "Generation of intense uv radiation by subharmonically seeded single-pass free-electron lasers," *Phys. Rev. A* **44**, 5178–5193 (1991).
- E. Allaria, R. Appio, L. Badano, *et al.*, "Highly coherent and stable pulses from the FERMI seeded free-electron laser in the extreme ultraviolet," *Nat. Photonics* **6**, 699–704 (2012).
- J. Amann, W. Berg, V. Blank, *et al.*, "Demonstration of self-seeding in a hard-X-ray free-electron laser," *Nat. Photonics* **6**, 693–698 (2012).
- A. A. Lutman, T. J. Maxwell, J. P. MacArthur, M. W. Guetg, N. Berrah, R. N. Coffee, Y. Ding, Z. Huang, A. Marinelli, S. Moeller, and J. C. U. Zemella, "Fresh-slice multicolour X-ray free-electron lasers," *Nat. Photonics* **10**, 745–750 (2016).
- C. Emma, A. Lutman, M. W. Guetg, J. Krzywinski, A. Marinelli, J. Wu, and C. Pellegrini, "Experimental demonstration of fresh bunch self-seeding in an X-ray free electron laser," *Appl. Phys. Lett.* **110**, 154101 (2017).
- E. Ferrari, C. Spezzani, F. Fortuna, *et al.*, "Widely tunable two-colour seeded free-electron laser source for resonant-pump resonant-probe magnetic scattering," *Nat. Commun.* **7**, 10343 (2016).
- E. Hemsing, A. Halavanau, and Z. Zhang, "Enhanced self-seeding with ultrashort electron beams," *Phys. Rev. Lett.* **125**, 044801 (2020).
- K.-J. Kim, Y. Shvyd'ko, and S. Reiche, "A proposal for an X-ray free-electron laser oscillator with an energy-recovery linac," *Phys. Rev. Lett.* **100**, 244802 (2008).
- G. Marcus, A. Halavanau, Z. Huang, J. Krzywinski, J. MacArthur, R. Margraf, T. Raubenheimer, and D. Zhu, "Refractive guide switching a regenerative amplifier free-electron laser for high peak and average power hard x rays," *Phys. Rev. Lett.* **125**, 254801 (2020).
- R. Alonso-Mori, D. Sokaras, M. Cammarata, *et al.*, "Femtosecond electronic structure response to high intensity XFEL pulses probed by iron X-ray emission spectroscopy," *Sci. Rep.* **10**, 1–7 (2020).
- T. Fransson, R. Alonso-Mori, R. Chatterjee, *et al.*, "Effects of x-ray free-electron laser pulse intensity on the Mn K $\beta_{1,3}$  x-ray emission spectrum in photosystem II-A case study for metalloprotein crystals and solutions," *Struct. Dyn.* **8**, 064302 (2021).
- T. Hara, Y. Inubushi, T. Katayama, T. Sato, H. Tanaka, T. Tanaka, T. Togashi, K. Togawa, K. Tono, M. Yabashi, and T. Ishikawa, "Two-colour hard X-ray free-electron laser with wide tunability," *Nat. Commun.* **4**, 2919 (2013).
- I. Inoue, T. Osaka, T. Hara, and M. Yabashi, "Two-color X-ray free-electron laser consisting of broadband and narrowband beams," *J. Synchrotron Radiat.* **27**, 1720–1724 (2020).
- I. Inoue, T. Osaka, T. Hara, *et al.*, "Generation of narrow-band X-ray free-electron laser via reflection self-seeding," *Nat. Photonics* **13**, 319–322 (2019).

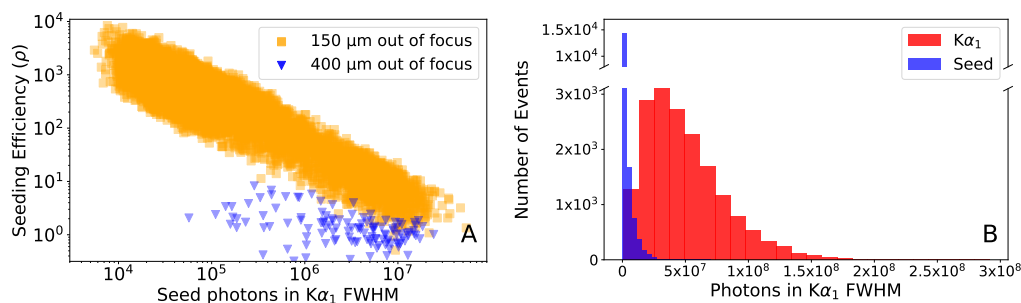


**Fig. 5.** (a) Seeding efficiency as a function of seed photon counts that fall within the spectral range of  $K\alpha_1$  FWHM for two different pump intensities. Shots are displayed for cases where the seed is in the range of  $\delta E = [0, +7]$  eV for the case of 150  $\mu\text{m}$  out of focus, and  $\delta E = [0, +2]$  eV for the case of 400  $\mu\text{m}$  out of focus. (b) Photon count distribution of  $K\alpha_1$  and seed pulse photons from a seeded scan at 150  $\mu\text{m}$  out of focus, at a pump pulse intensity of  $1.1 \times 10^{18}$  W/cm $^2$ .

30. T. Osaka, I. Inoue, R. Kinjo, *et al.*, "A micro channel-cut crystal X-ray monochromator for a self-seeded hard X-ray free-electron laser," *J. Synchrotron Radiat.* **26**, 1496–1502 (2019).
31. M. Yabashi, H. Tanaka, and T. Ishikawa, "Overview of the SACLA facility," *J. Synchrotron Radiat.* **22**, 477–484 (2015).
32. K. Tono, T. Togashi, Y. Inubushi, T. Sato, T. Katayama, K. Ogawa, H. Ohashi, H. Kimura, S. Takahashi, K. Takeshita, H. Tomizawa, S. Goto, T. Ishikawa, and M. Yabashi, "Beamline, experimental stations and photon beam diagnostics for the hard X-ray free electron laser of SACLA," *New J. Phys.* **15**, 083035 (2013).
33. H. Yumoto, Y. Inubushi, T. Osaka, I. Inoue, T. Koyama, K. Tono, M. Yabashi, and H. Ohashi, "Nanofocusing optics for an X-ray free-electron laser generating an extreme intensity of 100 EW/cm<sup>2</sup> using total reflection mirrors," *Appl. Sci.* **10**, 2611 (2020).
34. K. Tono, "Fluid sample injectors for X-ray free electron laser at SACLA," *High Power Laser Sci. Eng.* **5**, e7 (2017).
35. T. Katayama, S. Owada, T. Togashi, K. Ogawa, P. Karvinen, I. Vartiainen, A. Eronen, C. David, T. Sato, K. Nakajima, Y. Joti, H. Yumoto, H. Ohashi, and M. Yabashi, "A beam branching method for timing and spectral characterization of hard X-ray free-electron lasers," *Struct. Dyn.* **3**, 034301 (2016).
36. I. Inoue, Y. Inubushi, T. Osaka, J. Yamada, K. Tamasaku, H. Yoneda, and M. Yabashi, "Shortening x-ray pulse duration via saturable absorption," *Phys. Rev. Lett.* **127**, 163903 (2021).
37. T. Ida, M. Ando, and H. Toraya, "Extended pseudo-Voigt function for approximating the Voigt profile," *J. Appl. Crystallogr.* **33**, 1311–1316 (2000).
38. D. F. Hotz, "Gain narrowing in a laser amplifier," *Appl. Opt.* **4**, 527–530 (1965).
39. A. Halavanau, M. Doyle, A. Aquila, *et al.*, "Progress report on population inversion x-ray laser oscillator at LCLS," in *International Particle Accelerator Conference* (JACoW Publishing, 2022), Vol. **13**, pp. 1107–1109.